



Effect of Mn substitution on the cation distribution and temperature dependence of magnetic anisotropy constant in $\text{Co}_{1-x}\text{Mn}_x\text{Fe}_2\text{O}_4$ ($0.0 \leq x \leq 0.4$) ferrites

M. Atif^{a,b,*}, R. Sato Turtelli^b, R. Grössinger^b, M. Siddique^c, M. Nadeem^d

^aDepartment of Physics, Air University, PAF Complex E-9, Islamabad, Pakistan

^bInstitute of Solid State Physics, Technical University of Vienna, A-1040 Vienna, Austria

^cPhysics Division, PINSTECH, PO Nilore, Islamabad, Pakistan

^dElectronic and Magnetic Materials Group, PD, PINSTECH, PO Nilore, Islamabad, Pakistan

Received 19 April 2013; received in revised form 5 June 2013; accepted 10 June 2013

Available online 17 June 2013

Abstract

The effect of Mn substitution on temperature dependent magnetic properties of Mn substituted cobalt ferrite, i.e., $\text{Co}_{1-x}\text{Mn}_x\text{Fe}_2\text{O}_4$ ($x=0.0-0.4$), prepared by a ceramic method has been investigated. X-ray diffraction (XRD) analysis reveals that all samples possess a single phase cubic spinel structure. The lattice constant determined from XRD increases with Mn substitution whereas the bulk density of the samples decreases. Mössbauer results reveal that Co, Fe and Mn ions are distributed over the tetrahedral (A) and octahedral (B) sites for the prepared samples. Hysteresis loops yield a saturation magnetization (M_s) and coercive field (H_c) that vary significantly with temperature and Mn content (x). The temperature dependence of the magnetization obtained for $\mu_0 H = 5$ T presents a maximum at 175 K which is also dependent on the value of x . The high field regimes of the hysteresis loops are modeled using the Law of Approach to Saturation (LAS) to determine the first-order cubic anisotropy coefficient (K_1). It has been found that the anisotropy of these materials increases significantly with decreasing temperature. However, below 175 K, the shape of the anisotropy energy function changes significantly causing a first-order magnetization process (FOMP) at higher fields, which also prevents the magnetization to saturate even under a maximum applied field of 5 T. In general, the anisotropy coefficient decreases with increasing Mn substitution at a given temperature, which could be explained in terms of the site occupancy of the Mn^{2+} substituent in the cubic spinel lattice.

© 2013 Elsevier Ltd and Techna Group S.r.l. All rights reserved.

Keywords: A. Milling; B. Spectroscopy; C. Magnetic properties; D. Ferrites

1. Introduction

Cobalt ferrite, CoFe_2O_4 , is a well-known hard magnetic material, which has been extensively studied due to their interesting properties such as high cubic magnetocrystalline anisotropy, high coercivity, good electrical insulation, high chemical stability, significant mechanical hardness and moderate saturation magnetization at room temperature [1–3]. However, the increasing interest in cobalt ferrite and cobalt

ferrite based materials is mainly due to their strong magnetoelastic effects and their potential usefulness in developing robust magnetoelastic stress sensors and energy efficient actuators [4,5]. Cobalt ferrite has a partially inverse spinel structure in which both sites, i.e. tetrahedral (A) and octahedral (B) sites, contain a fraction of Co^{2+} and Fe^{3+} cations; however it is generally accepted that a large fraction of Co^{2+} ions are on the B-site and the remaining are on the A-site, which depends on the production methods as well as on the heat treatment procedure [6–8]. Also, it is well known that the magnetic properties of cobalt ferrite depend on the concentration of Co^{2+} at B-site of the spinel structure. Therefore any changes in the site occupancy of Co^{2+} cation and/or deviation of targeted composition from stoichiometry (CoFe_2O_4) caused by cation

*Corresponding author at: Department of Physics, Air University, PAF Complex E-9, Islamabad, Pakistan. Tel.: +92 51 9262557 480; fax: +92 51 9260158.

E-mail addresses: matif_80@yahoo.com, atifip@gmail.com (M. Atif).

substitution or heat treatment will affect the physical properties of cobalt ferrite including the temperature dependence of magnetic properties and magnetomechanical hysteresis [9–11].

Recently, the temperature dependence of the magnetic anisotropy of a series of mixed ferrites $\text{CoM}_x\text{Fe}_{2-x}\text{O}_4$ ($M=\text{Mn, Cr, Ga}$ and Al) has been investigated [12–15] and it was found that substituting M for Fe in cobalt ferrite allows adjustment of the Curie temperature (T_c) of the material, thereby influencing the temperature dependence of its stress sensitivity and magnetomechanical response of these materials. It has been shown that manganese substituted cobalt ferrites, i.e. $\text{CoMn}_x\text{Fe}_{2-x}\text{O}_4$, are excellent candidates for stress sensors due to a large magnetomechanical effect and high sensitivity to stress. This is because weakening of the exchange coupling results in a decrease of the magnetocrystalline anisotropy which also results in a steeper response of strain to applied magnetic field [16]. From the studies on the magnetic and magnetostrictive properties of Mn substituted cobalt ferrites [16–18], it has been found that substitution of Mn enhances the saturation magnetization as well as the magnetostrictive properties of the cobalt ferrite; when Mn is substituted by Co in the B-site as compared to the displacement of Co from the B- to A-sites when Mn is substituted by Fe in the Co–Mn ferrite ($0.0 \leq x \leq 0.4$) system. This is because; the high magnetocrystalline anisotropy of the cobalt ferrite is due to the Co at B-site. However, it has been reported in our recent study [19] that the direct substitution of Mn for Co in the cobalt ferrite, i.e., $\text{Co}_{1-x}\text{Mn}_x\text{Fe}_2\text{O}_4$, showed a comparatively higher magnetostriction and strain derivative at relatively low magnetic fields for a peculiar composition, which depicts the importance of Mn substitution for Co in tuning the magnetoelastic response of cobalt ferrite [20]. Since, the temperature dependence of the magnetoelastic properties is strongly dependent on the magnetostriction and magnetic anisotropy, as well as coercivity, permeability, and chemical composition of the material. Therefore, it would be interesting to study the effect of substitution of Mn for Co instead of Fe in CoFe_2O_4 on the temperature dependent magnetic anisotropy and coercive field for the Mn substituted cobalt ferrites (i.e. $\text{Co}_{1-x}\text{Mn}_x\text{Fe}_2\text{O}_4$). In the present work, we report a systematic study on the crystal structure and magnetocrystalline anisotropy at various temperatures (i.e. 10–400 K) of Mn substituted cobalt ferrites $\text{Co}_{1-x}\text{Mn}_x\text{Fe}_2\text{O}_4$ for $0.0 \leq x \leq 0.4$ prepared under optimum synthesis conditions [9].

2. Experimental

A series of manganese substituted cobalt ferrite samples with compositions of $\text{Co}_{1-x}\text{Mn}_x\text{Fe}_2\text{O}_4$ ($x=0.0, 0.2, 0.4$) were prepared by ball milling technique. The process involved mixing of Fe_2O_3 , Co_3O_4 and MnO_2 powders in their stoichiometric amounts and then ball milled by using Spex 8000 high-energy vibratory mill for 8 h, followed by calcinations at 900°C for 12 h. To have better homogeneity in the samples, the powders were re-milled with intermediate annealing at 1000°C for 12 h and then the powders were pressed under a hydrostatic pressure of 167 MPa. Finally the pressed pellets

were sintered at 1350°C for 24 h and were subsequently furnace cooled to room temperature.

XRD patterns (obtained from the pellet surfaces) were recorded by means of an Xpert Philips diffractometer (Goniometer Philips PW3050/60) using $\text{CuK}_{\alpha 1,2}$ radiation in a Bragg Brentano geometry and a X'Celerator detector. The X-ray generator Philips PW 3040/60 worked at a power of 40 kV and 40 mA, and the goniometer was equipped with a graphite monochromator. Diffraction patterns were recorded in the angular range $15\text{--}90^\circ$ with a scan step size of 0.02° . Collected data were refined using the Rietveld package TOPAS (Bruker AXS Topas V 2.1) based on the fundamental parameter approach, with diffractometer parameters and wavelength settings adjusted using a LaB6 standard. The sintered pellets of all samples were properly ground for collecting room temperature Fe^{57} Mössbauer spectra. Co^{57} (Rh-matrix) source was used in transmission mode. $\alpha\text{-Fe}$ foil was used for the Mössbauer spectrometer calibration. Data were analyzed using the MOS-90 computer program by assuming all peaks as Lorentzian in shape. For the magnetic characterization, temperature dependent hysteresis loop measurements applying a maximum magnetic field of 5 T ($1\text{ T} \approx 796\text{ kA/m}$) were performed using a vibrating sample magnetometer (PPMS-VSM) from Quantum Design Inc.

3. Result and discussion

3.1. Structural analysis

Fig. 1 illustrates the XRD pattern of the Mn substituted cobalt ferrite sample with $x=0.4$ (i.e., $\text{Co}_{0.6}\text{Mn}_{0.4}\text{Fe}_2\text{O}_4$). All samples present similar XRD patterns, as shown in Fig. 1. XRD analysis followed by a Rietveld refinement based on the fundamental parameter approach shows that all peaks in Fig. 1

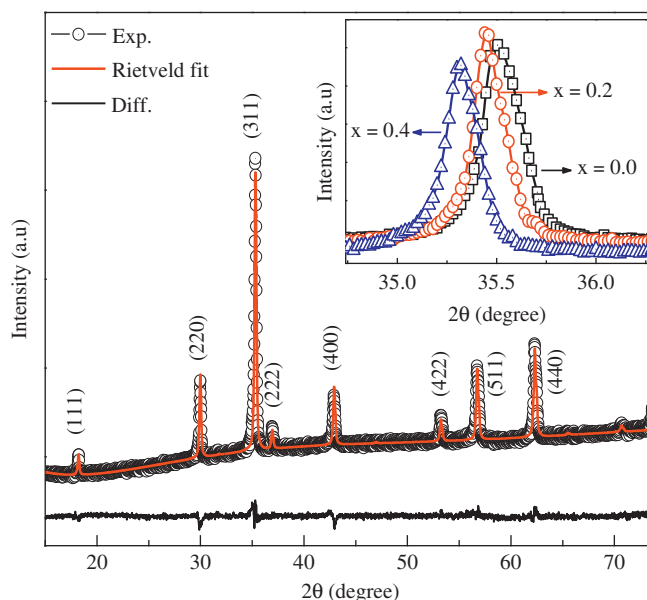


Fig. 1. X-ray diffraction patterns (experimental and Rietveld refinement) of $\text{Co}_{0.6}\text{Mn}_{0.4}\text{Fe}_2\text{O}_4$ sample sintered at 1350°C for 24 h. Inset shows the enlarged (311) XRD peaks for $\text{Co}_{1-x}\text{Mn}_x\text{Fe}_2\text{O}_4$ samples.

correspond to the characteristic peaks of ferrite material where (311) represents the most intense peak, which confirms the formation of cubic spinel structure. Here the open circles indicate experimental data, solid line represents Rietveld refined data and the bottom line shows the difference between the experimental and refined data. Inset of Fig. 1 shows a typical zoom of (311) XRD peak for the $\text{Co}_{1-x}\text{Mn}_x\text{Fe}_2\text{O}_4$ samples. From the inset, a shift in the (311) peak positions can be observed indicating that the lattice constant changes systematically due to the Mn substitution. The lattice constant 'a', determined from XRD data, increases with increasing Mn content from 8.3826 Å to 8.4213 Å as 'x' varies from 0.0 to 0.4 in $\text{Co}_{1-x}\text{Mn}_x\text{Fe}_2\text{O}_4$. The increase of lattice constant is attributed to the replacement of smaller ionic radius of Co^{2+} (0.78 Å) by the larger Mn^{2+} (0.83 Å) ions in the $\text{Co}_{1-x}\text{Mn}_x\text{Fe}_2\text{O}_4$ system [21]. Similar variation of lattice constant is reported in the literature for the $\text{Co}_{1-x}\text{Mn}_x\text{Fe}_2\text{O}_4$ spinel ferrite [18,22]. The crystallite size (the volume averaged size of the coherently diffracting domains) was obtained from X-ray diffraction line broadening by means of Rietveld refinement. The average crystallite sizes vary in the range of 102–125 nm (± 3) with increase in Mn content (Table 1). The X-ray density D_x of the prepared samples was calculated from the XRD patterns, whereas the bulk density D_s was calculated from the geometry and mass of the samples. Since, density is inversely proportional to the lattice constant, it decreases as the lattice constant increases [23]. Accordingly from Table 1, it can be observed that the value of D_x and D_s decreases with Mn substitution. This may be due to the fact that the density and atomic weight of Mn are smaller than that of Co ions. However, the smaller value of D_s than that of the D_x is due to the existence of pores that depend on the sintering and pressing conditions. The variation of the porosity of samples with composition is also given in Table 1. The porosity of the samples increases with composition; this may be due to the release of oxygen from the samples during sintering i.e., the decrease in oxygen ion (anion) diffusion would retard the densification [24].

3.2. Mössbauer spectroscopy

In order to study the possibility of structural changes and coordination differences of iron in the $\text{Co}_{1-x}\text{Mn}_x\text{Fe}_2\text{O}_4$ samples, room temperature ^{57}Fe Mössbauer spectroscopy has been used. Mössbauer spectra of the prepared samples are shown in Fig. 2. For all three samples, the Mössbauer spectrum can be well fitted with a regular magnetic sextet whereas the line

width shows the presence of two distinct six line hyperfine patterns. The parameters associated with two sextets are typical for iron ions in the tetrahedral (A-site) and octahedral (B-site) coordination. The Mössbauer parameters, i.e. isomer shift (δ), quadrupole splitting (Δ), hyperfine field (H_{eff}) and resonance area (RA) obtained from the fitting of Mössbauer spectra are presented in Table 2. The line width of the B-site becomes broader than that of the A-site with increasing Mn content. Such broadening is, in fact, expected due to a distribution of hyperfine fields caused by a random distribution of Co^{2+} , Mn^{2+} and Fe^{3+} ions at the A- and B-sites [25]. The observed values of quadrupole splitting (Δ) of all samples investigated here are found to be almost zero. Therefore, there is no distortion in the overall cubic symmetry between Fe^{3+} ions and their surroundings by substituting Mn^{2+} ions in cobalt ferrites. In addition, the values of isomer shifts (δ) of the A- and B-sites do not vary with Mn^{2+} content. The range of values of the isomer shift indicates that iron exists in the Fe^{3+} valence state with a high spin configuration in the prepared samples [26]. However, the smaller value of A-site isomer shift compared to B-site is due to a large covalent contribution at the A-site [27].

The addition of Mn^{2+} in $\text{Co}_{1-x}\text{Mn}_x\text{Fe}_2\text{O}_4$ causes a variation of the hyperfine field (H_{eff}) and resonance area (RA) of the A- and B-sites (see Table 2). In most of the ferrites, the B-site hyperfine magnetic field is generally larger than that of the

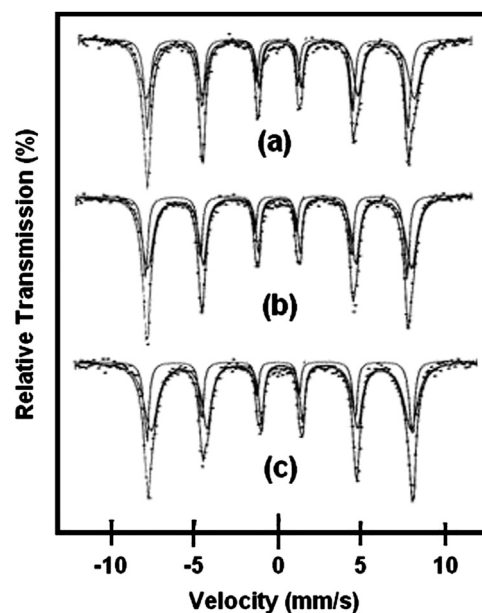


Fig. 2. Mössbauer spectra of $\text{Co}_{1-x}\text{Mn}_x\text{Fe}_2\text{O}_4$ samples for (a) $x=0.0$, (b) $x=0.2$ and (c) $x=0.4$ recorded at room temperature.

Table 1

Composition dependence of the lattice constant (a), crystallite size (t), X-ray density (D_x), bulk density (D_s), porosity (P), magnetization (M) at 300 K, coercivity (H_c) at 300 K, Curie temperature (T_c) and anisotropy constant (K_1) at 300 K for $\text{Co}_{1-x}\text{Mn}_x\text{Fe}_2\text{O}_4$.

Composition (x)	a (Å)	t (nm)	D_x (g/cm ³)	D_s (g/cm ³)	P (%)	M (kA/m)	H_c (kA/m)	T_c (K)	$K_1 \times 10^5$ (J/m ³)
$x=0.0$	8.382	102	5.291	4.935	6.7	419	11	784	3.81
$x=0.2$	8.397	116	5.263	4.694	10.8	427	7	750	2.91
$x=0.4$	8.421	125	5.218	4.269	18.6	434	2	695	1.82

Table 2
Mössbauer parameters, hyperfine magnetic field (H_{eff}), quadrupole splitting (Δ), isomer shift (δ), Line width (Γ) and relative area (RA) of $\text{Co}_{1-x}\text{Mn}_x\text{Fe}_2\text{O}_4$ ($x=0.0, 0.2, 0.4$) ferrites.

Sample (x)	Site	H_{eff} (kOe)	Δ (mm/s)	δ (mm/s)	Γ (mm/s)	RA (%)
0.0	A	495	0.00	0.23	0.40	41
	B	510	0.00	0.40	0.87	59
0.2	A	493	0.00	0.20	0.35	34
	B	497	0.00	0.40	0.80	66
0.4	A	492	0.05	0.23	0.35	30
	B	482	-0.07	0.38	0.98	70

A-site, because of the larger covalency at the A-site [25,27]. Whereas, the relative area under the resonance curve of the sub-spectra deduced from the measurements is used to estimate the Fe occupancy for each site. It can be seen from Table 2 that there is no significant variation in the hyperfine interaction at the A-site (i.e., 495–492 kOe) with Mn substitutions, whereas the hyperfine interaction at B-site is found to decrease from 510 to 482 kOe with increasing Mn substitution. The observed decrease in the hyperfine field at the B-site with increasing Mn^{2+} substitution in $\text{Co}_{1-x}\text{Mn}_x\text{Fe}_2\text{O}_4$ is due to the migration of Fe^{3+} ions from A- to B-sites, as Mn^{2+} ions has preference for A-site [22]. Moreover, it has been found that the relative peak area of the B-site increases and that of A-site decreases accordingly, with the substitution of Mn ions. This variation in relative peak area is related to the fact that the intensity of the outer sextet increases while that of inner sextet decreases with the substitution of Mn ions (see Fig. 2). We have calculated the cation distribution of different compositions from the relative peak area and the ratio of A-site sextet intensity to that of B-site, which is summarized in Table 3. The estimated cation distributions show that the structure is really that of a mixed spinel phase where Co, Fe and Mn ions are distributed in a nonstatistic way over the A- and B-sites (see Table 3), which is in accordance with the previous reports based on the Mössbauer studies of ferrite systems [28,29]. However, a slight difference in the estimated values of cation distribution is attributed to the different production method and also on heat treatment procedure. Therefore, the cation distribution produces a significant effect on the magnetic properties, which is discussed in the next section.

3.3. Magnetic studies

Fig. 3(a–c) shows the magnetic hysteresis loops for $\text{Co}_{1-x}\text{Mn}_x\text{Fe}_2\text{O}_4$ ($x=0.0, 0.2, 0.4$) samples measured at different temperatures ranging from 10 to 400 K, with a maximum applied field of 5 T. With increasing temperature the hysteresis loops becomes magnetically softer over the whole temperature range for all samples with different Mn content. However, for temperatures below 200 K, it can be seen from the left inset of

Table 3
Cation distribution in the spinel structure as estimated by Mössbauer spectroscopy for the samples $\text{Co}_{1-x}\text{Mn}_x\text{Fe}_2\text{O}_4$ ($x=0.0, 0.2, 0.4$) and calculation of the accordingly resulting moment M_B-M_A .

Samples	A-site	B-site	M_B-M_A (μ_B)
CoFe_2O_4	$\text{Co}_{0.18}\text{Fe}_{0.82}$	$\text{Co}_{0.82}\text{Fe}_{1.18}$	3.72
$\text{Co}_{0.8}\text{Mn}_{0.2}\text{Fe}_2\text{O}_4$	$\text{Co}_{0.16}\text{Mn}_{0.16}\text{Fe}_{0.68}$	$\text{Co}_{0.64}\text{Mn}_{0.04}\text{Fe}_{1.32}$	4.03
$\text{Co}_{0.6}\text{Mn}_{0.4}\text{Fe}_2\text{O}_4$	$\text{Co}_{0.08}\text{Mn}_{0.32}\text{Fe}_{0.60}$	$\text{Co}_{0.52}\text{Mn}_{0.08}\text{Fe}_{1.40}$	4.12

Fig. 3(a–c) that the magnetization of the sample could not saturate in the available field of 5 T. This is an indication that the anisotropy is so high that higher magnetic fields are required to saturate the samples. In order to elucidate this detail, the temperature dependence of the magnetization curve was obtained in a zero-field cooling mode (ZFC), as shown in Fig. 4(a). In ZFC measurements, the samples were cooled from room temperature to 10 K without applying an external magnetic field. After reaching 10 K, a 5 T field is applied and then magnetization was recorded as the temperature was increased. It can be seen from Fig. 4(a) that initially magnetization increases as temperature increased from 10 to 100 K for all samples. Above 100 K, magnetization increases slowly with increasing temperature for $x=0.0$ and $x=0.2$ samples but decreases for $x=0.4$ sample (from 110 K), $x=0.2$ (from 150 K) and $x=0.0$ (from 175 K). This apparent increase in the magnetization at low temperatures can be explained by the presence of an anisotropy anomaly in high fields at low temperatures for these samples, which prevent complete saturation of magnetization under the field strengths used. It is worth to note that in pure CoFe_2O_4 single crystal a field induced first-order phase transition (FOMP) occurs at about 6 T (at $T=10$ K) [30]. Therefore also in polycrystalline material at fields below this critical field no saturation can be achieved. From these measurements, it can be also seen that the magnetization increases due to the substitution of Mn^{2+} for Co^{2+} in CoFe_2O_4 . The observed variation in the magnetization can be explained due to the difference in the contributions from the magnetic moment of the substituted ion on the A- and

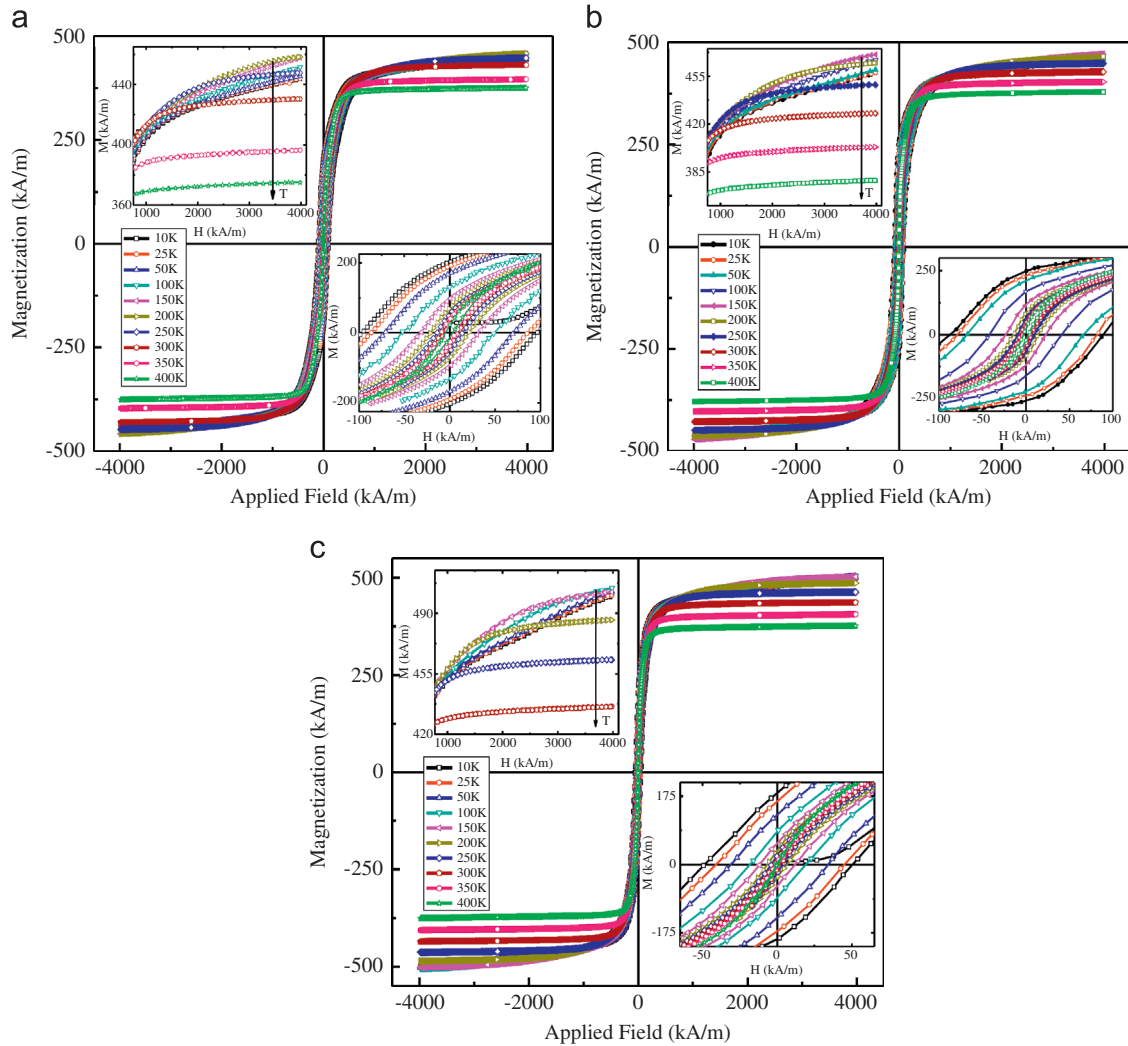


Fig. 3. Hysteresis loops for $\text{Co}_{1-x}\text{Mn}_x\text{Fe}_2\text{O}_4$ samples (a) $x=0.0$ (b) $x=0.2$ (c) $x=0.4$, obtained at several temperatures (10–400 K). Left insets of each figure shows the high field regions of hysteresis loops, and right insets shows the low field regions of hysteresis loops used to calculate coercivity.

B-sites of the spinel ferrite (i.e. total magnetization $M_T = M_B - M_A$). In $\text{Co}_{1-x}\text{Mn}_x\text{Fe}_2\text{O}_4$ system, an increase in the magnetization is expected after the substitution of Mn for Co if Co^{2+} (d^7) replaced by Mn^{2+} (d^5), since Mn^{2+} has a larger magnetic moment of $5 \mu_B$ as compared with $3 \mu_B$ for Co^{2+} . In this work, as was deduced from Mössbauer results, Mn^{2+} ions are partially distributed in both A- and B-sites of mixed spinel cobalt ferrite having preference for A-site, then such distribution affects the M_T value. The determined values of M_T increases with Mn substitution as shown in Table 3. In the present study the small increase in the total magnetization due to the migration of Fe^{3+} ions from the A to the B-sites, as was shown by the Mossbauer results (see Table 3) caused by the substitution of Mn^{2+} in the $\text{Co}_{1-x}\text{Mn}_x\text{Fe}_2\text{O}_4$ system from $x=0.0$ to $x=0.4$ concentration value is in agreement with the reported values [17,20].

The Curie temperature, T_c , was also measured by applying a magnetic field of 5 T and heating the samples from room temperature through the Curie temperature at a rate of 5 K/min. As expected the magnetization decreased with increasing

temperature approaching to zero near the Curie temperature, i.e. at ≈ 784 K for $x=0.0$, which is in good agreement with that previously reported for Co-ferrite [31]. The inset of Fig. 4(b) shows the variation of the first derivative of the magnetization (dM/dT) versus absolute temperature for the $x=0.2$ sample from which the Curie temperature (T_c) was calculated for different Mn contents. It is evident that substituting Mn for Co in cobalt ferrite reduced the Curie temperature T_c linearly (see Table 1), which may be attributed to the decrease in the strength of the exchange interaction constant J_{AB} . However, the observed increase in the magnetization marginally prevents the predominant A–B exchange interaction from weakening and thus explains the slow decrease of the Curie temperature (up to $x \leq 0.4$).

The coercive fields H_c at different temperatures as calculated from the hysteresis loops are shown in Fig. 5. With increasing temperature monotonic decreasing coercivity has been observed for all samples. The decrease in coercivity with increasing temperature can be explained by considering the effects of thermal fluctuations of the blocked moment across

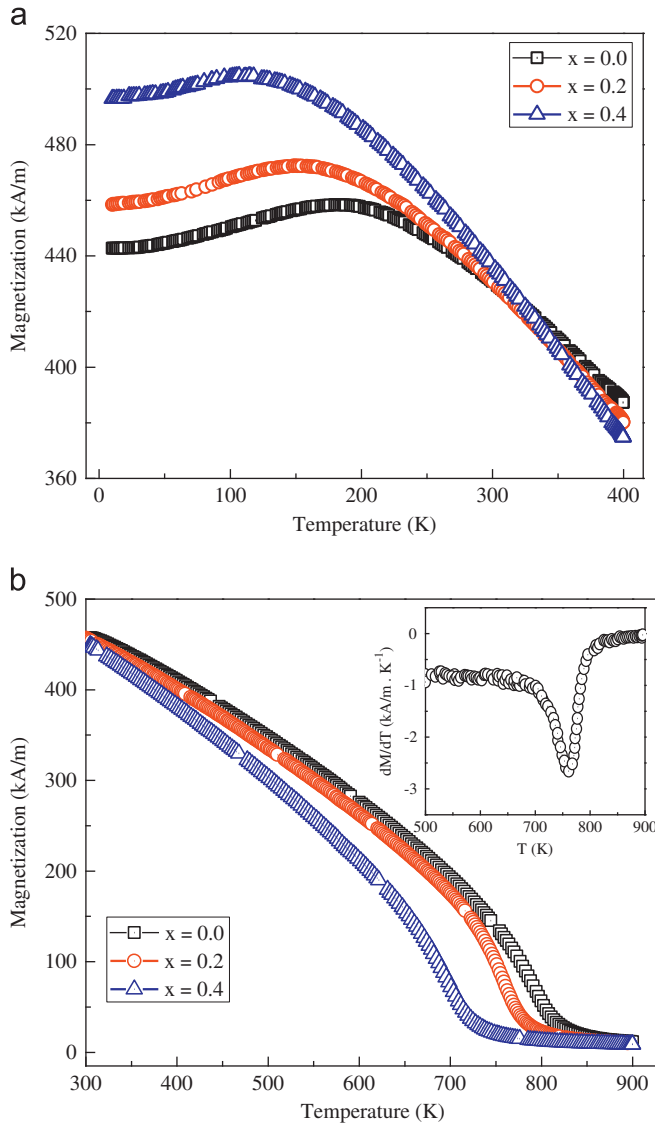


Fig. 4. Temperature dependence of magnetization measured (a) varying temperature from 10 K to 400 K in a zero-field cooling (ZFC) mode and (b) varying temperature from 300 K to 900 K for $\text{Co}_{1-x}\text{Mn}_x\text{Fe}_2\text{O}_4$ at an applied field of 5 T. Inset of (b) shows a first derivative of magnetization for $x=0.2$ sample.

the anisotropy barrier. Since, coercivity in a ferrite system is known to depend on several parameters such as anisotropy constant, lattice imperfections, internal strains and grain size etc. In the present $\text{Co}_{1-x}\text{Mn}_x\text{Fe}_2\text{O}_4$ system, it can be seen that the coercivity decreases more rapidly for $x=0.4$ as compared with $x=0.2$, which may be attributed to some extrinsic parameters such as microstructures (increased porosity) and large grain size [19] apart from the reduction in anisotropy due to the increased presence of Mn^{2+} ions in $\text{Co}_{1-x}\text{Mn}_x\text{Fe}_2\text{O}_4$. However, it should be mentioned here that the observed coercivity variation invariably points out that the variation in the net anisotropy in the system due to the presence of Mn^{2+} ions is the dominant mechanism responsible for determining the other parameters discussed above.

In order to extract the temperature dependence of anisotropy information of the prepared samples i.e. $\text{Co}_{1-x}\text{Mn}_x\text{Fe}_2\text{O}_4$

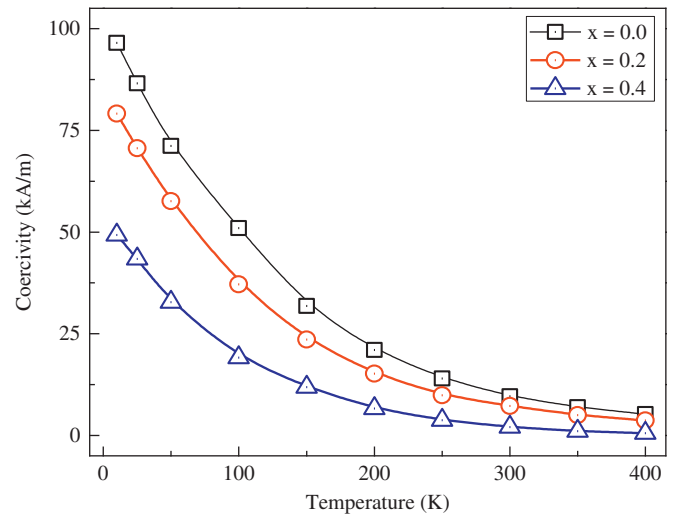


Fig. 5. Temperature dependence of coercivity for the $\text{Co}_{1-x}\text{Mn}_x\text{Fe}_2\text{O}_4$ samples.

($x=0.0, 0.2, 0.4$), the Law of Approach to Saturation (LAS) was applied to analyze the data in the saturated region. LAS describes the dependence of magnetization M on the applied magnetic field for $H \gg H_c$ assuming only rotational processes. The magnetization near M_s is usually written as [32]

$$M(H) = M_s(1 - b/H^2) + \kappa H \quad (1)$$

where M is the magnetization, H is the applied magnetic field, M_s is the saturation magnetization and $b = 8 K_1^2 / 105 \mu_0^2 M_s^2$ for randomly oriented polycrystalline samples with a cubic crystal structure [33]. The term κH is caused by an increase in the spontaneous magnetization itself especially at high fields and is known as the forced magnetization, where the parameter κ is the high-field susceptibility. Therefore, M_s , K_1 , and κ are the fitting parameters remaining in Eq. 1. For the fitting process, magnetization curves with fields higher than 3 T ($H > H_c$) are used for the temperatures $T \leq 175$ K; whereas for temperatures above 175 K, only the parts of magnetization curves with fields higher than 1.5 T are fitted to the LAS (Eq. 1) in order to extract the most appropriate values of K_1 , M_s , and κ . From the analysis of this fitting process, it has been found that for temperatures $T \leq 175$ K, M_s and K_1 are the only fitting parameters as detailed examination of the curves revealed that the forced magnetization is negligible in this region, therefore $\kappa=0$ is chosen at these temperatures. It should be mentioned that due to the occurrence of a FOMP at higher fields [30], the calculated value of the “saturation magnetization” is too small. Generally M_s increases with decreasing temperature from 400 to 175 K for all samples (see Fig. 6). The values of M_s , computed by fitting Eq. (1) to the experimental data, are found to be approximately the same as that measured from the maximum magnetization measured at 5 T for these temperatures. Whereas below 175 K, the fitted values for M_s are due to the FOMP below the true saturation magnetization. In this case the maximum applied field is no longer able to saturate these samples at these temperature, thus indicating that complex

anisotropy behavior (FOMP) determines the $M(H)$ behavior at low temperatures [12,30].

Fig. 7 shows the temperature dependence of the cubic anisotropy constant K_1 estimated by Eq. 1 for $\text{Co}_{1-x}\text{Mn}_x\text{Fe}_2\text{O}_4$ ($x=0.0, 0.2, 0.4$). It can be seen that the anisotropy constant K_1 is strongly dependent on temperature as well as on Mn contents whereas the values of K_1 are of the order of 10^5 J/m^3 which are comparable with the reported values [10,12–14,30]. For all Mn substituted cobalt ferrites, K_1 increases first with increasing temperature starting from 10 K, however this increase is smaller for the $x=0.4$ sample and it appears to level off at the lowest temperatures for the sample $x=0.4$; whereas it appears to increase for the sample with $x=0.2$ and $x=0.0$. As mentioned already these anomalous increases are due to the critical FOMP field which is larger than 5 T. This causes a

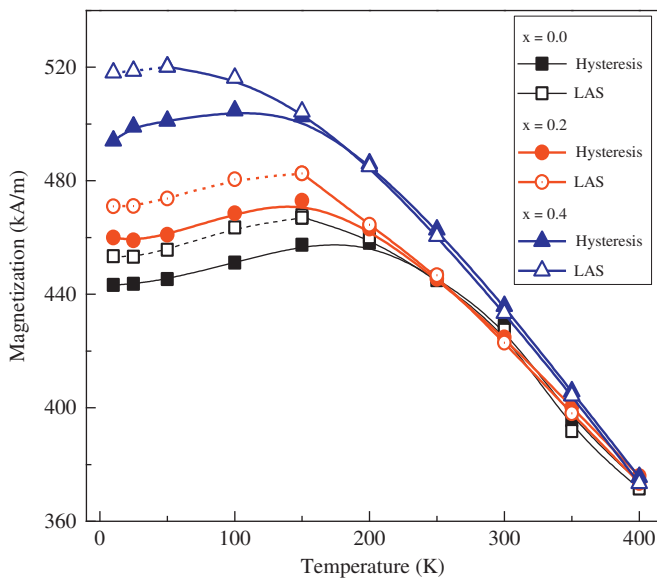


Fig. 6. Temperature dependence of magnetization for $\text{Co}_{1-x}\text{Mn}_x\text{Fe}_2\text{O}_4$ samples obtained by fitting Eq. (1) and experimental $M(H)$ data (Fig. 3).

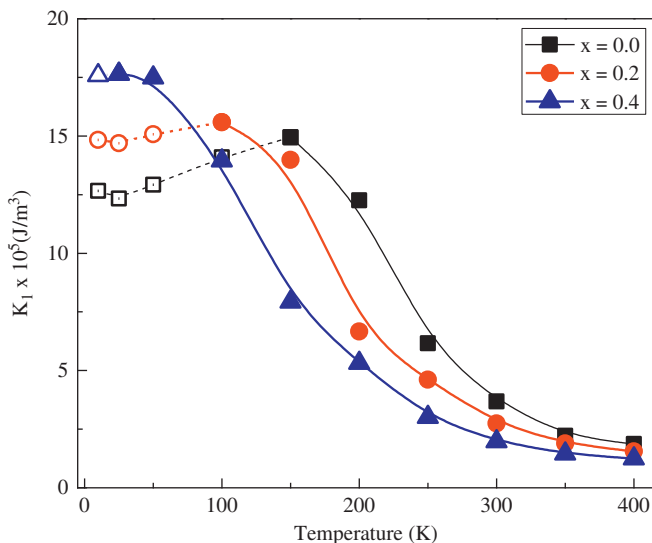


Fig. 7. Temperature dependence of the anisotropy constant K_1 for $\text{Co}_{1-x}\text{Mn}_x\text{Fe}_2\text{O}_4$ samples determined using $M(H)$ data.

$M(H)$ curve at low temperatures which is not simply determined by K_1 . Additionally the anisotropy fields $\mu_0 H_K = 2 K_1 / M_s$ [6] of these samples reaches very high values at low temperatures (i.e. below 175 K). In this case the applied fields of $\mu_0 H = 5 \text{ T}$ is far away from a saturated state of the material (see Fig. 2). At such temperatures, the values of K_1 calculated from fitting the experimental data to the LAS equation are unreliable, even if calculated with the force magnetization coefficient set to zero, i.e., $\kappa=0$. However, in the relatively high temperature region (i.e. above 175 K), the anisotropy of all the Mn substituted cobalt ferrites (i.e. $x=0.0, 0.2, 0.4$) decreases substantially with increasing temperature. For this region, the maximum applied field is sufficiently large compared to the anisotropy field for these temperatures (due to a decreasing ratio of exchange interaction to thermal energy) and this allows us to apply the LAS successfully. In the present study, for temperatures above 175 K, the estimated values of cubic anisotropy constant K_1 for these ferrites is consistent with the experimental data for pure single crystals of cobalt ferrites measured by a modified torque magnetometer method by Shenker [34] and by the theoretical work of Tachiki [35]. And they are still the same order of magnitude and follow the same trend, i.e., K_1 decreases with increasing temperature.

The composition dependence of the anisotropy of Mn substituted cobalt ferrite can be understood due to the effect of Mn substitution on the site occupancies of the cations. It is known that the strong anisotropy of cobalt ferrite is primarily due to the presence of Co^{2+} ions on the B-site of the spinel structure [36]. The results of our current studies of the Mn substituted cobalt ferrites suggest that, although the Co^{2+} ions occupy both A- and B-sites, the B-site is most populated by Co^{2+} ions causing an increase in anisotropy. However with the substitution of Mn^{2+} for Co^{2+} , it has been found Co^{2+} ions are replaced by Mn^{2+} at both A- and B-sites. Since Mn^{2+} ions has stronger preference for A-site which in turn pushes Fe^{3+} ions from A- to B-sites which results in the reduction of magnetocrystalline anisotropy found for all temperatures $> 175 \text{ K}$ where a good agreement with LAS could be obtained.

4. Conclusions

The effect of Mn substitution on the temperature dependence of the magnetic anisotropy, magnetization, and coercivity of cobalt ferrite $\text{Co}_{1-x}\text{Mn}_x\text{Fe}_2\text{O}_4$ for $x=0.0, 0.2, 0.4$ has been investigated over the temperature range of 10–400 K. Mössbauer measurements show well resolved magnetic spectra for the tetrahedral and octahedral sites. Cation distribution estimated from Mössbauer spectroscopy revealed that Co^{2+} , Fe^{3+} and Mn^{2+} ions are randomly distributed over the A- and B-sites. The observed variations in magnetization and Curie temperature are explained on the basis of cation site occupancies and the strength of the exchange interactions; whereas coercivity decreases with Mn content which is attributed to anisotropic nature of Co ions. The magnetocrystalline anisotropy coefficient, K_1 , is obtained by fitting the high-field parts of the hysteresis loop using $M(H)$ data with the LAS equation. It is found that K_1 increases with decreasing temperature for all

Mn substituted cobalt ferrites. The observed decrease with increasing Mn content is interpreted in terms of a cation redistribution between the A- and B-sites of the spinel structure of cobalt ferrite. Also, due to the fact that the prepared samples exhibit a high K_1 at low temperatures, much higher fields ($\mu_0 H > 5$ T) are required to saturate the magnetization. This can be explained by the FOMP transition at higher fields found in pure CoFe_2O_4 . Therefore, in these cases K_1 cannot be calculated correctly by LAS method at low temperature.

Acknowledgment

M. Atif would like to thank Higher Education Commission (HEC) of Pakistan for providing financial support under Overseas Scholarship Scheme (Phase-II) for Ph.D. studies.

References

- [1] J.P. Jakubovics, in: *Magnetism and Magnetic Materials*, Cambridge University Press, London, 1994.
- [2] Y. Köseoğlu, M.I.O. Olewi, R. Yilgin, A.N. Koçbay, Effect of chromium addition on the structural, morphological and magnetic properties of nano-crystalline cobalt ferrite system, *Ceramics International* 38 (2012) 6671–6676.
- [3] A. Berkovitz, W.T. Schuele, Magnetic properties of some ferrite micropowders, *Journal of Applied Physics* 30 (1959) S134.
- [4] R.W. McCallum, K.W. Dennis, D.C. Jiles, J.E. Snyder, Y.H. Chen, Composite magnetostrictive materials for advanced automotive magnetomechanical sensors, *Low Temperature Physics* 27 (2001) 266.
- [5] Y. Chen, J.E. Snyder, C.R. Schwichtenberg, K.W. Dennis, R.W. McCallum, D.C. Jiles, Metal-bonded Co-ferrite composites for magnetostrictive torque sensor applications, *IEEE Transactions on Magnetics* 35 (1999) 3652–3654.
- [6] B.D. Cullity, *Introduction to Magnetic Materials*, Addison-Wisley, USA, 1972.
- [7] R. Sato Turtelli, M. Atif, N. Mehmood, F. Kubel, K. Biernacka, W. Linert, R. Grössinger, Cz. Kapusta, M. Sikora, Interplay between the cation distribution and production methods in cobalt ferrite, *Materials Chemistry and Physics* 132 (2012) 832–838.
- [8] N. Kasapoğlu, A. Baykal, Y. Köseoğlu, M.S. Toprak, Microwave-assisted combustion synthesis of CoFe_2O_4 with urea, and its magnetic characterization, *Scripta Materialia* 57 (2007) 441–444.
- [9] I.C. Nlebedim, J.E. Snyder, A.J. Moses, D.C. Jiles, Dependence of the magnetic and magnetoelastic properties of cobalt ferrite on processing parameters, *Journal of Magnetism and Magnetic Materials* 322 (2010) 3938–3942.
- [10] A. Muhammad, R. Sato-Turtelli, M. Kriegisch, R. Grössinger, F. Kubel, T. Konegger, Large enhancement of magnetostriction due to compaction hydrostatic pressure and magnetic annealing in CoFe_2O_4 , *Journal of Applied Physics* 111 (2012) 013918.
- [11] Y. Köseoğlu, F. Alan, M. Tan, R. Yilgin, M. Öztürk, Low temperature hydrothermal synthesis and characterization of Mn doped cobalt ferrite nanoparticles, *Ceramics International* 38 (2012) 3625–3634.
- [12] Y. Melikhov, J.E. Snyder, D.C. Jiles, A.P. Ring, J.A. Paulsen, C.C.H. Lo, K.W. Dennis, Temperature dependence of magnetic anisotropy in Mn-substituted cobalt ferrite, *Journal of Applied Physics* 99 (2006) 08R102.
- [13] Y. Melikhov, J.E. Snyder, C.C.H. Lo, P.N. Matlage, S.H. Song, K.W. Dennis, D.C. Jiles, The effect of Cr-substitution on the magnetic anisotropy and its temperature dependence in Cr-substituted cobalt ferrite, *IEEE Transactions on Magnetics* 42 (2006) 2861–2863.
- [14] N. Ranvah, Y. Melikhov, D.C. Jiles, J.E. Snyder, A.J. Moses, P. I. Williams, S.H. Song, Temperature dependence of magnetic anisotropy of Ga-substituted cobalt ferrite, *Journal of Applied Physics* 103 (2008) 07E506.
- [15] N. Ranvah, I.C. Nlebedim, Y. Melikhov, J.E. Snyder, P.I. Williams, A. J. Moses, D.C. Jiles, Temperature dependence of magnetic properties of $\text{CoAl}_x\text{Fe}_{2-x}\text{O}_4$, *IEEE Transactions on Magnetics* 45 (2009) 4261–4264.
- [16] J.A. Paulsen, C.C.H. Lo, J.E. Snyder, A.P. Ring, L.L. Jones, D.C. Jile, Manganese-substituted cobalt ferrite magnetostrictive materials for magnetic stress sensor applications, *Journal of Applied Physics* 97 (2005) 044502.
- [17] S.D. Bhame, P.A. Joy, Enhanced magnetostrictive properties of Mn substituted cobalt ferrite $\text{Co}_{1.2}\text{Fe}_{1.8}\text{O}_4$, *Journal of Applied Physics* 99 (2006) 073901.
- [18] R.C. Kambale, P.A. Shaikh, N.S. Harale, V.A. Bilur, Y.D. Kolekar, C.H. Bhosale, K.Y. Rajpure, Structural and magnetic properties of $\text{Co}_{1-x}\text{Mn}_x\text{Fe}_2\text{O}_4$ ($0 \leq x \leq 0.4$) spinel ferrites synthesized by combustion route, *Journal of Alloys and Compounds* 490 (2010) 568–571.
- [19] M. Atif, R. Sato-Turtelli, R. Grössinger, F. Kubel, Influence of manganese substitution on the microstructure and magnetostrictive properties of $\text{Co}_{1-x}\text{Mn}_x\text{Fe}_2\text{O}_4$ ($x=0.0-0.4$) ferrite, *Journal of Applied Physics* 113 (2013) 153902.
- [20] S.D. Bhame, P.A. Joy, Magnetic and magnetostrictive properties of manganese substituted cobalt ferrite, *Journal of Physics D: Applied Physics* 40 (2007) 3263–3267.
- [21] K.J. Standley, *Oxide Magnetic Materials*, Clarendon Press, Oxford, 1972.
- [22] D.H. Lee, H.S. Kim, C.H. Yo, K. Ahn, K.H. Kim, The magnetic properties and electrical conduction mechanism of $\text{Co}_{1-x}\text{Mn}_x\text{Fe}_2\text{O}_4$ spinel, *Materials Chemistry and Physics* 57 (1998) 169–172.
- [23] C. Venkataraju, Effect of nickel on the structural properties of Mn Zn ferrite nanoparticles, *Applied Physics Research* 1 (2009) 41–45.
- [24] T. Abbas, M.U. Islam, M.A. Choudhury, Study of sintering behavior and electrical properties of Cu–Zn–Fe–O system, *Modern Physics Letters B* 9 (1995) 1419–1426.
- [25] A.M. Gismelseed, A.A. Yousif, Mössbauer study of chromium-substituted nickel ferrites, *Physica B* 370 (2005) 215–222.
- [26] D.P.E. Dickson, F.J. Berry, in: *Mössbauer Spectroscopy*, Cambridge University Press, London, 1986.
- [27] K.P. Thummer, M.C. Chhantbar, K.B. Modi, G.J. Baldha, H.H. Joshi, ^{57}Fe Mössbauer studies on $\text{MgAl}_x\text{Cr}_y\text{Fe}_{2-2x}\text{O}_4$ spinel system, *Materials Letters* 58 (2004) 2248–2251.
- [28] G.A. Sawatzky, F. Van Der Woude, A.H. Morish, Mössbauer study of several ferrimagnetic spinels, *Physical Review* 187 (1969) 747–757.
- [29] V.K. Singh, N.K. Khatri, S. Lokanathan, Mossbauer study of ferrite systems $\text{Co}_x\text{Mn}_{1-x}\text{Fe}_2\text{O}_4$ and $\text{Ni}_x\text{Mn}_{1-x}\text{Fe}_2\text{O}_4$, *Pramana* 16 (1981) 273–280.
- [30] M. Kriegisch, W. Ren, R. Sato Turtelli, H. Müller, R. Grössinger, Z. Zhang, Field-induced magnetic transition in cobalt-ferrite, *Journal of Applied Physics* 111 (2012) 07E308.
- [31] J. Smit, H.P.J. Wijn, *Ferrites—Physical Properties of Ferrimagnetic Oxides in Relation to Their Technical Applications*, N.V. Philips Gloeilampenfabrieken, Eindhoven/Holland, 1959.
- [32] S. Chikazumi, in: *Physics of Magnetism*, Wiley, New York, 1964.
- [33] R.M. Bozorth, in: *Ferromagnetism*, IEEE, New York, 1993.
- [34] H. Shenker, Magnetic anisotropy of cobalt ferrite ($\text{Co}_{1.01}\text{Fe}_{2.03}\text{O}_{3.62}$) and nickel cobalt ferrite ($\text{Ni}_{0.72}\text{Fe}_{0.20}\text{Co}_{0.08}\text{Fe}_2\text{O}_4$), *Physical Review* 107 (1957) 1246–1249.
- [35] M. Tachiki, Origin of the Magnetic Anisotropy Energy of Cobalt Ferrite, *Progress of Theoretical Physics* 23 (1960) 1055–1072.
- [36] J.C. Slonczewski, Origin of magnetic anisotropy in cobalt-substituted magnetite, *Physical Review* 110 (1958) 1341–1348.